



Dynamics of charge carrier trapping in NO₂ sensors based on ZnO field-effect transistors

Anne-Marije Andringa^{a,b,*}, Nynke Vlietstra^{a,b}, Edsger C.P. Smits^c, Mark-Jan Spijkman^{a,b}, Henrique L. Gomes^d, Johan H. Klotwijk^b, Paul W.M. Blom^{a,c}, Dago M. de Leeuw^{a,b,**}

^a University of Groningen, Zernike Institute for Advanced Materials, Nijenborgh 4, 9747 AG Groningen, The Netherlands

^b Philips Research Laboratories, High Tech Campus 4, 5656 AE Eindhoven, The Netherlands

^c Holst Centre, High Tech Campus 31, 5656 AE Eindhoven, The Netherlands

^d Universidade do Algarve, Faculty of Science and Technology, Campus de Gambelas, 8005-139 Faro, Portugal

ARTICLE INFO

Article history:

Received 27 March 2012

Received in revised form 1 June 2012

Accepted 22 June 2012

Available online 1 July 2012

Keywords:

NO₂ sensors

Field-effect transistor

Charge carrier trapping

Threshold voltage shift

Stretched-exponential

Thermally stimulated current

Activation energy

ABSTRACT

Nitrogen dioxide (NO₂) detection with ZnO field-effect transistors is based on charge carrier trapping. Here we investigate the dynamics of charge trapping and recovery as a function of temperature by monitoring the threshold voltage shift. The threshold voltage shifts follow a stretched-exponential time dependence with thermally activated relaxation times. We find an activation energy of 0.1 eV for trapping and 1.2 eV for detrapping. The attempt-to-escape frequency and characteristic temperature have been determined as 1 Hz and 960 K for charge trapping and 10¹¹ Hz and 750 K for recovery, respectively. Thermally stimulated current measurements confirm the presence of trapped charge carriers with a trap depth of around 1 eV. The obtained functional dependence is used as input for an analytical model that predicts the sensor's temporal behavior. The model is experimentally verified and a real-time sensor has been developed. The perfect agreement between predicted and measured sensor response validates the methodology developed. The analytical description can be used to optimize the driving protocol. By adjusting the operating temperature and the duration of charging and resetting, the response time can be optimized and the sensitivity can be maximized for the desired partial NO₂ pressure window.

© 2012 Elsevier B.V. All rights reserved.

1. Introduction

NO₂ sensors are required to monitor and control air-quality. Commercial sensors are typically chemiresistors, which monitor changes in grain boundary resistances [1–3]. In recent years, field-effect transistors have been suggested as an alternative sensing technology [4,5]. A wide variety of semiconductors has been investigated for NO₂ sensing, such as amorphous organic semiconductors [6,7], porous silicon [8,9], silicon nanowires [10], carbon nanotubes [11–13], and metal oxide nanowires [14]. In all cases, changes in current upon NO₂ exposure have been demonstrated. In addition, a high sensitivity down to 10 ppb NO₂ has been reported.

The detection mechanism has been elucidated using ZnO as a semiconductor [15]. The electrical transport does not change when the transistor is exposed to NO₂. However, the transport changes

in an NO₂ ambient *when a gate bias is applied*. A current decrease in time is observed, originating from a shift of the threshold voltage towards the applied gate bias. The rate of the threshold voltage shift depends on the partial NO₂ pressure. Concentrations as low as 10 ppb can be detected.

A typical response of a ZnO transistor exposed to an NO₂ ambient is presented in the 3D plot of Fig. 1a. A constant gate bias was applied and after certain time intervals the linear transfer curves were measured. The transfer curves shift with stress time in the direction of the applied gate bias. As a result, the source–drain current decreases and eventually becomes equal to the leakage current. The complete transfer curve shifts without changing shape, indicating that the mobility is not affected. The main effect of NO₂ exposure is a shift of the threshold voltage, V_{th} , here empirically defined as the onset of current flow [16]. In Fig. 1a, the red line shows the threshold voltage shift towards the applied gate bias as a function of stress time on a semi-logarithmic scale. The origin of the shift is trapping of charge carriers [15]. The gate bias sets the total accumulated charge density. As elucidated in Fig. 1b, with time carriers are getting trapped, the density of free carriers decreases and the current drops. At infinite time all carriers are trapped, leading to a negligible current and a threshold voltage equal to the applied gate bias.

* Corresponding author at: Philips Research Laboratories, High Tech Campus 4, 5656 AE Eindhoven, The Netherlands. Tel.: +31 402742547.

** Corresponding author at: Philips Research Laboratories, High Tech Campus 4, 5656 AE Eindhoven, The Netherlands. Tel.: +31 402742547.

E-mail addresses: annemarije.andringa@gmail.com (Anne-Marije Andringa), dago.de.leeuw@philips.com (D.M. de Leeuw).

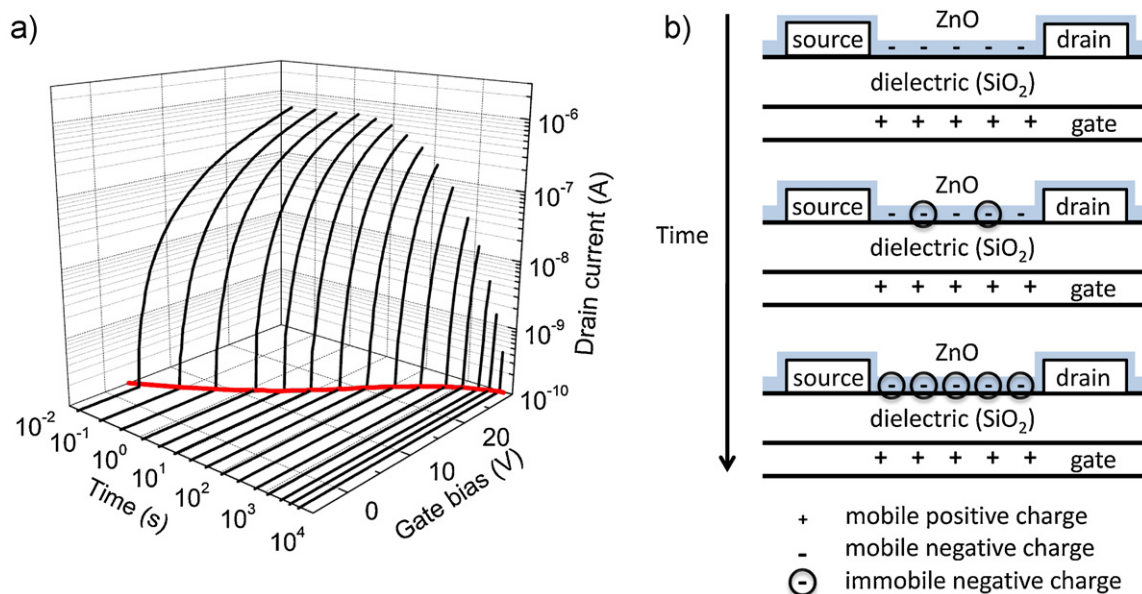


Fig. 1. (a) Transfer curves of a ZnO transistor exposed to 320 ppb NO_2 , as a function of time under a continuously applied gate bias of 30 V. The linear transfer curves, represented by the black lines, were measured at a source–drain bias of 2 V. The red line presents the threshold voltage as a function of stress time. The threshold voltage is empirically taken as the onset of current flow. The threshold voltage starts at about 0 V and shifts with time towards the applied gate bias of 30 V. (b) Schematic representation of the charge trapping process in a transistor. With time, mobile electrons are trapped until the steady-state is reached. The gate bias is then completely compensated by immobile trapped charges. (For interpretation of the references to color in this figure legend, the reader is referred to the web version of the article.)

The change in current or threshold voltage with time depends on the NO_2 concentration. Hence a field-effect transistor can in theory be used as an NO_2 sensor. At room temperature however the charge trapping is irreversible. The time scale for release of charge carriers, or recovery, is larger than days. In other words, at room temperature the transistor is not a sensor but an integrator as it monitors the accumulation of trapped charge carriers. The response of a sensor to an analyte should be reversible, which implies that the time scales for trapping and release of charge carriers should be comparable. Here we investigate the dynamics of charge trapping and recovery as a function of temperature. We show that at each temperature, the threshold voltage shifts follow a stretched-exponential time dependence. The relaxation times are thermally activated. The activation energies for trapping and release are independent of the NO_2 content and determined as 0.1 eV and 1.2 eV respectively. The values for the corresponding attempt-to-escape frequencies and characteristic temperatures are discussed. The activation energy for charge release is also determined by thermally stimulated current (TSC) measurements, yielding a value of approximately 1 eV. The good agreement confirms that charge carrier trapping is the responsible mechanism of the threshold voltage shift. In the final part, the experimentally determined threshold voltage dynamics is used as input for an analytical model that predicts the sensor's temporal behavior. The response of the transistor can be calculated without any additional fit constants. We show that a sensor protocol can be made that allows for a dynamic read-out of the partial NO_2 pressure in real time. The model is experimentally verified and a real-time sensor is developed.

2. Experimental

The fabrication and characterization of unipolar *n*-type ZnO field-effect transistors has been described in detail in Ref. [15]. Briefly, transistor test structures were fabricated on heavily doped *n*-type Si wafers, acting as common gate electrode, with a 200 nm thermally oxidized SiO_2 layer as gate dielectric. Gold source and drain electrodes were defined by conventional photolithography, resulting in interdigitated transistors with a channel length of

10 μm and a width of 10,000 μm . The ZnO was applied using spray pyrolysis in ambient atmosphere [17]. A solution of zinc acetate in methanol was nebulized and deposited on top of the transistor substrate, heated at 400 °C. The transistor geometry is schematically depicted in Fig. 1b. The ZnO layers were characterized with X-ray fluorescence (XRF), X-ray diffraction (XRD), and atomic force microscopy (AFM). The morphology of the ZnO films was microcrystalline with a surface roughness of 1 nm (root mean square (rms)). XRD measurements showed that the ZnO films exhibited a (1 0 2) textured microstructure. The film thickness of the mirror-like ZnO films was only 10 nm to ensure permeability for NO_2 . To reduce the surface conductivity of the ZnO layer, a self-assembled-monolayer (SAM) of *n*-octadecyl phosphonic acid was applied from a 3 mM ethanol solution. The SAM was tested to have no effect on the sensitivity towards NO_2 . The passivated ZnO transistors had a field-effect mobility of 0.1–2 $\text{cm}^2 \text{V}^{-1} \text{s}^{-1}$ and showed negligible hysteresis and high stability under gate bias stress.

The sensor's response to NO_2 was tested in a flow system equipped with feedthroughs for the electrical contacts. The temperature of the heater, electrically insulated from the transistor substrate by a thin sheet of Mica, was regulated using a Eurotherm 2416 controller. NO_2 was supplied from a cylinder containing 3 ppm NO_2 in N_2 as carrier gas (Praxair). The partial NO_2 pressure was lowered by dilution with pure N_2 . Two mass flow controllers were used to regulate the NO_2 concentration. The actual NO_2 concentration in the gas flow was measured continuously with an Eco Physics CLD 88p NO sensor. A gas converter of M&C (type CG) was used to convert NO_2 catalytically to NO at 330 °C with a carbon molybdenum mixture. The transistor was stable in NO_2 without applying a gate bias. Therefore, electrical measurements were performed in a stabilized NO_2 concentration that was reached after 30 min flow.

Gate bias stress measurements were carried out using a Keithley 2602A System SourceMeter controlled by an in-house developed Labview program. To reduce charge trapping during the probing of the threshold voltage, the transfer curves were measured in less than a second by implementing a compliance stop at 100 nA. The ZnO transistors were annealed in vacuum at 150 °C in order to

set the threshold voltage at 0 V before each measurement. As the threshold voltage we take the gate bias at which the source drain current is 1 nA. The TSC measurements were conducted in sampling mode with an Agilent 4155B Semiconductor Parameter Analyzer using an integration time of 0.5 s.

3. Threshold voltage dynamics

To investigate the trapping dynamics in a ZnO field-effect transistor, stress and recovery measurements were performed as a function of temperature. The partial NO₂ pressure was fixed at approximately 1.1 ppm. Fig. 2a shows the threshold voltage as a function of time during stress with a continuous applied gate bias at various temperatures. The solid lines are fits of the data to a stretched-exponential time dependence:

$$\Delta V_{th}(t) = V_0 \left\{ 1 - \exp \left[- \left(\frac{t}{\tau} \right)^\beta \right] \right\} \quad (1)$$

where τ is a relaxation time, the dispersion parameter β equals T/T_0 , and $V_0 = V_G - V_{th0}$, where V_G is the applied gate bias and V_{th0} is the threshold voltage at the start of the experiment. A good agreement between measured data and the fits is obtained. The inset in Fig. 2a shows the extracted dispersion parameter β as a function of temperature. A linear dependence is obtained

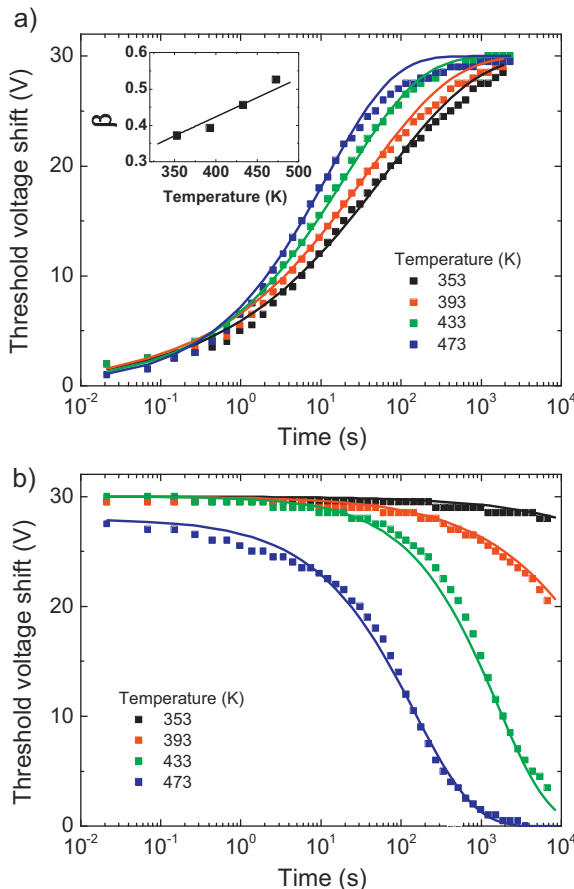


Fig. 2. (a) Threshold voltage shift of a ZnO field-effect transistor in NO₂ as a function of time under continuous applied gate bias of 30 V for several temperatures. The NO₂ concentration was approximately 1.1 ppm. The solid lines are fits with a stretched-exponential time dependence. The inset shows the dispersion parameter β as a function of temperature. (b) Temperature dependence of the threshold voltage shift in recovery. The threshold voltage was first set at 30 V by applying a continuous gate bias. With the NO₂ still present, the stressed transistors were recovered by grounding both gate and drain electrodes. The threshold voltage shift as a function of time was fitted with a stretched exponential.

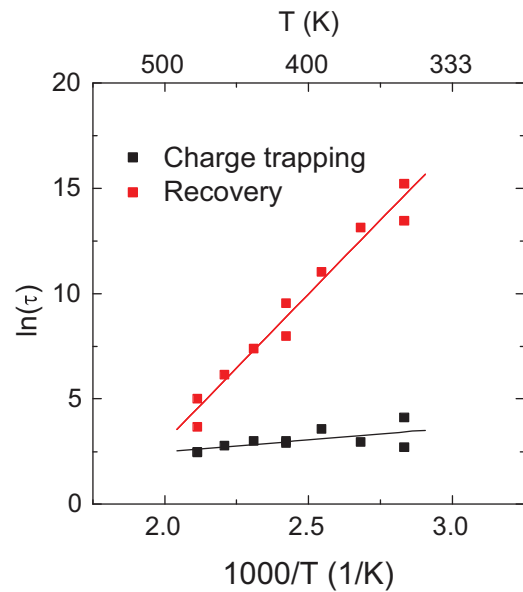


Fig. 3. Relaxation times, τ , as a function of reciprocal temperature for charge trapping and recovery. The solid lines show that τ is thermally activated for both stress and recovery with activation energies of 0.1 eV and 1.2 eV, respectively. The attempt-to-escape frequencies are 1 Hz and 10¹¹ Hz respectively.

with a characteristic temperature of T_0 of 950 ± 75 K. The charge trapping hardly depends on temperature. The relaxation time for charge trapping, τ , is presented in Fig. 3 as a function of reciprocal temperature (black). A straight line is obtained, showing that the relaxation time is thermally activated as:

$$\tau = \nu^{-1} \exp \left(\frac{E_a}{k_B T} \right) \quad (2)$$

with a small activation energy, E_a , of 0.10 ± 0.04 eV and an attempt-to-escape frequency, ν , of 1 ± 1 Hz. We note that the attempt-to-escape frequency is equal to the phonon frequency multiplied by the probability of electron–phonon colocalization [18].

The recovery of the threshold voltage was measured as a function of temperature. First the threshold voltage was set at 30 V by applying a continuous gate bias. With the NO₂ still present, the stressed transistors were then recovered by grounding both gate and drain electrodes. The resulting threshold voltage shifts as a function of time for various temperatures are presented in Fig. 2b. The solid lines are fits with a stretched-exponential time dependence (Eq. (1)). A good agreement is obtained. The characteristic temperature, T_0 , is experimentally difficult to determine. We estimate a temperature around 750 K, comparable to the characteristic temperature extracted from the stress measurements. Fig. 2b shows that the detrapping becomes much faster with increasing temperature. The extracted relaxation time, τ , is presented in Fig. 3 as a function of reciprocal temperature (red). The activation energy for detrapping amounts to 1.2 ± 0.1 eV and an attempt-to-escape frequency, ν , is derived of $10^{11 \pm 1}$ Hz.

The relaxation time for charge trapping was found to be inversely proportional to the NO₂ pressure [15]. At low NO₂ content the measurement takes hours to days. The long time scale hampers a reliable determination of the activation energy. Within experimental accuracy however there is no change; the activation energy is expected to be independent on the partial NO₂ pressure. Recovery has been investigated with and without NO₂ present and furthermore in N₂ and compressed dry air. The activation energy for charge detrapping did not depend on the ambient.

In recovery we investigated the changes in threshold voltage shift due to the applied biases. For drain biases between 0 V and

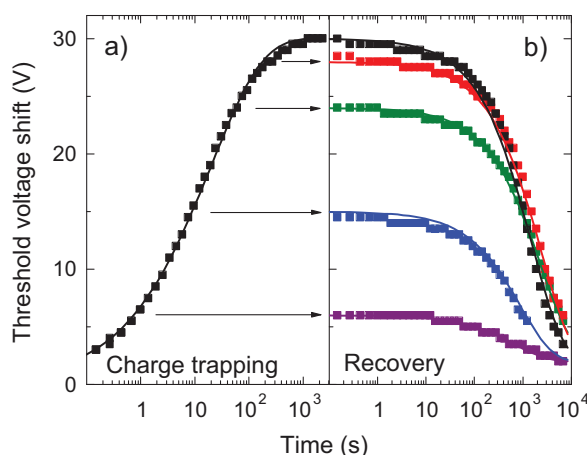


Fig. 4. (a) Threshold voltage of a ZnO field-effect transistor in NO_2 as a function of time under a continuous applied gate bias of 30 V. (b) After a certain stress time, varied between 1 s and 2000 s, the gate bias was set to 0 V and the recovery was measured, as indicated by the arrows. The solid lines are fitted with a stretched-exponential time dependence. The relaxation times obtained do not depend on the history.

20 V there is hardly any change in relaxation time. Similarly, the relaxation time was not affected by the value of the applied gate bias. Only the final threshold voltage changes; it saturates at the applied positive gate bias. Furthermore, the recovery could not be enhanced by putting the stressed transistor in deep depletion by applying a negative gate bias. A parameter that influences the kinetics is the presence of light. It has been reported that the recovery properties of ZnO and SnO_2 sensors were improved remarkably by UV light irradiation [19–21]. Preliminary experiments show that the relaxation time under UV illumination in the ZnO FET decreases by orders of magnitude.

The operational reliability of organic and inorganic field-effect transistors has been studied extensively. It has been reported that the time scale for recovery then depends on the extent of stressing [22]. Here we have investigated the recovery of the ZnO transistors as a function of the trapped charge density. Fig. 4a shows the threshold voltage of a ZnO transistor in an NO_2 ambient as a function of stress time using a 30 V gate bias. After a certain stress time, varied between 1 s and 2000 s, the gate bias was set to 0 V and the recovery was measured. The solid lines in Fig. 4b are fitted with a stretched-exponential time dependence. The relaxation times obtained did not depend on the history, viz. the trapped charge density. The reason is not yet understood.

4. Thermally stimulated current

To confirm the presence of trapped charge carriers and to derive the trap density and energetic depth, thermally stimulated current measurements were performed. The traps are filled by applying a bias while the temperature is such that the trapped carriers cannot be freed by the thermal energy. The temperature is then raised linearly. The liberated carriers contribute to the excess current, i.e. the external current minus the leakage current, until they recombine with carriers of opposite type or join the equilibrium charge carrier distribution. This excess current, measured as function of temperature during heating, is called the thermally stimulated current. For a single trap level, a TSC curve has one maximum whose position depends on capture cross section, heating rate and trap depth. By varying the heating rates the trap depth and capture cross-section can also be determined. Because detrapping currents are extremely small (pA), TSC can only be used with relatively insulating materials. Gate bias-stressed TFTs satisfy

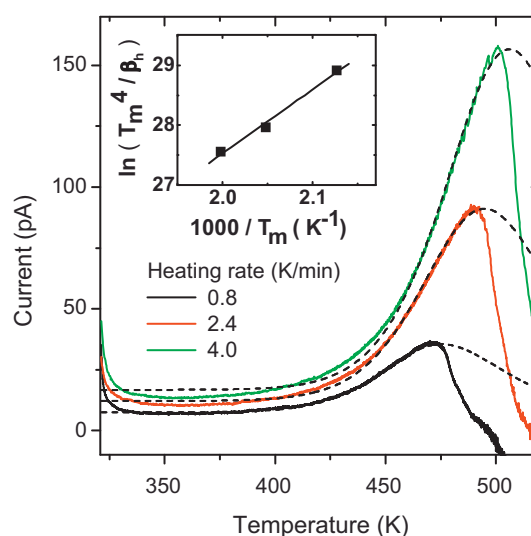


Fig. 5. Thermally stimulated current as a function of temperature (TSC) obtained in a ZnO field-effect transistor exposed to 1.1 ppm NO_2 . The traps were filled at 320 K by applying a 30 V gate bias for 1300 s and grounding the source and drain electrodes. After stressing the source and drain current was measured while grounding all three electrodes. The heating rates, β_h , were 0.8, 2.4 and 4.0 K/min. The dashed lines are a fit to the data using the Cowell and Woods method. The inset presents a plot of $\ln(T_m^4 / \beta_h)$ versus T_m^{-1} , where T_m is the temperature of the current maximum.

this requirement because they behave as normally off or fully depleted TFTs. When performing TSC experiments the transistor is connected as a metal–insulator–semiconductor (MIS) capacitor.

A transistor is exposed to 1.1 ppm NO_2 and a gate bias of 30 V is applied for 1300 s. The transfer curve then is fully shifted to the applied gate bias; all induced accumulated carriers are trapped. The trap filling was performed at room temperature, detrapping can be disregarded (Fig. 2b). The stressed transistor then is heated at a constant rate, $\beta_h = dT/dt$, up to 520 K. The trapped carriers are released and collected at the grounded source and drain electrodes. The temperature where a current peak occurs is related to the energetic depth of the trap state and the area under the peak is related to the trap density.

The TSC curves as a function of temperature are presented in Fig. 5 for three linear heating rates, 0.8, 2.4 and 4.0 K/min. The TSC gradually increases with temperature until a peak maximum is observed at a particular temperature, T_m . Both the absolute value of the current and T_m increase with the heating rate as expected.

The density of filled traps, N_t , can be estimated from the time integrated TSC current as:

$$Q = eN_tA = \int I dt \quad (3)$$

where Q is the integrated total charge and A is the surface area between the electrodes. However, experimentally we do not observe a linear dependence of the integrated current on the channel length, which indicates that the charges are extracted from an area larger than that between the electrodes. This conclusion is supported by the magnitude of the integrated current. The derived trapped charge density from the threshold voltage shift and the dielectric capacitance is 3×10^{12} charges per cm^2 . From the TSC measurements we arrive at an integrated total charge of 9×10^{-8} C. Assuming that only the area between the electrodes contributes to the TSC current, we calculate a trapped charge density of 6×10^{14} charges per cm^2 . The value is two orders of magnitude higher. The reason for this discrepancy lies in the fact that the entire substrate is coated with ZnO. Therefore, when the gate bias is applied, the entire ZnO/ SiO_2 interface is charged. The charges in the vicinity of the TFT can diffuse to the contacts and the leads, where they are

collected and measured in the external circuit. Based on the differences of the total amount of charge and the experimental device geometry we estimate that electrons can diffuse over distances in the order of 1 mm.

The extraction of the trap parameters from TSC measurements is not straightforward. The current temperature profile does not only depend on the density, depths and distribution of the traps, but depends also on the details of the charge transport such as charge carrier mobility and the occurrence of retrapping. The data was analyzed using several models, viz. the initial rise time method [23,24], the heating rate method [25,26] and the curve fitting method by Cowell and Woods [27,28].

The initial rise method is valid for all types of recombination kinetics and assumes that the current in the initial part of the curve, when the traps begin to empty, is exponentially dependent on temperature. This method is often used when the full TSC curve cannot be recorded or is distorted by other processes. The method only provides the trap depth and is usually less accurate than the other models. The initial TSC curves in Fig. 5 follow a single exponential behavior with an activation energy of 0.72 eV.

A more reliable determination of the trap depth is obtained from the relation between the heating rate β_h and the temperature of the peak maximum, T_m , as described by Blood and Orton in Eq. (4):

$$\ln \left\{ \frac{T_m^4}{\beta_h(T_m)} \right\} = \frac{\Delta E}{k_B T_m} + \ln \left(\frac{\Delta E}{\sigma \gamma k_B} \right) \quad (4)$$

in which β_h is the heating rate, ΔE is the trap depth, k_B is the Boltzmann constant, σ is the capture cross section and γ is a parameter depending on the effective mass. From the series of TSC scans at different heating rates in Fig. 5, the peak temperatures, T_m , are determined. The activation energy of the trap can then be obtained from a linear plot of $\ln(T_m^4/\beta_h)$ versus T_m^{-1} . The inset in Fig. 5 shows that a straight line is obtained. The slope yields a value for the activation energy, ΔE , of 0.92 eV.

Finally, we fitted the complete TSC curves numerically using the classical approach of Cowell and Woods. The underlying assumption is monomolecular recombination of the charge carriers from a discrete set of traps with a single trapping level with a trap depth ΔE below the conduction band, with negligible retrapping. The current then follows from:

$$I = \frac{A \exp(-\Theta)}{(1 + B \exp(-\Theta)\Theta^{-2})^2} + I_{off} \quad (5)$$

in which $A = n_t \tau e \mu \nu$, $B = \nu \Delta E / \beta_h k_B = \Theta_m^2 \exp \Theta_m$, $\Theta = \Delta E / kT$ and $\Theta_m = \Delta E / kT_m$. Here, n_t is the initial density of filled traps, τ is the average lifetime of a free carrier, μ is the mobility and ν is the attempt-to-escape frequency. The TSC curves can be fitted with four fitting parameters, T_m , A , ΔE and I_{off} . We note that at high temperatures, when a significant number of traps is emptied, the conductivity of the TFT channel is partially restored and the associated background current severely distorts the measurements. For temperatures above the TSC peak the current cannot be treated solely as a detrapping current and the analysis is not possible. The best fits, shown in Fig. 5 as dashed lines, show a good agreement with the measured currents. We extracted a trap depth ΔE of 1.0 eV comparable to the value derived by the method of Blood and Orton described above.

We can also estimate the apparent capture cross section (σ) as the attempt-to-escape frequency divided by the thermal velocity and the density of conduction band states (N_c). We note that when we assume that B equals $\nu \Delta E / \beta_h k_B$, we derive an attempt-to-escape frequency, ν , in the order of 10^7 Hz. Using a thermal velocity of 10^7 cm/s [29] and $N_c = 10^{20}$ cm $^{-3}$ we derive an apparent cross section in the order of 10^{-20} cm 2 . This small value might suggest that in order to capture a charge carrier, a repulsive barrier has

to be surmounted [25]. However, the attempt-to-escape frequency may be grossly underestimated because the fitting parameters are not independent. A more reasonable value for ν of 10^{11} Hz was obtained from the recovery measurements. By using this value the apparent cross section is estimated to be 10^{-16} cm 2 in line with a non-ionized, neutral trap.

5. Trapping mechanism

The different time constants for charge trapping and recovery can be explained by a deep trap filling process. The trap filling is essentially controlled by the number of unoccupied trap states and by the free carrier density induced by the gate bias, while the recovery is due to thermally activated emission. Initially, the transistor is not stressed. The traps are empty and the free carrier concentration is relatively high. The capture rate, c_n , is directly proportional to the free carrier concentration, n , and to the number of unoccupied states [30]:

$$c_n = n \{N_t [1 - f(E_t)]\} v_{th} \sigma_n \quad (6)$$

where $N_t [1 - f(E_t)]$ gives the density of empty states, N_t is the density of filled traps, E_t is the trap depth, v_{th} the thermal velocity and σ_n is the capture cross section. As the threshold voltage shifts towards the applied gate bias, the free carrier density decreases which slows down the capture rate. Eq. (6) shows that the capture rate is temperature independent. Only the thermal velocity depends on the square root of the absolute temperature. For the experimentally used temperature range of 300 K through 500 K, this dependence can be disregarded. In conclusion, the electron capture process is a temperature independent process as is experimentally observed by an almost negligible activation energy of 0.1 eV.

We note that the attempt-to-escape frequency of 1 Hz extracted from the threshold voltage dynamics upon charging is orders of magnitude lower than that of a typical phonon frequency of 10^{12} Hz. The reason is that depending on the microscopic mechanism, the extracted escape-frequency contains temperature independent prefactors. We conjecture that the rate determining step is the diffusion of NO $_2$ at the gate dielectric–ZnO interface. We have shown previously that the relaxation time τ then is inversely proportional to the density of NO $_2$ at the gate dielectric–ZnO interface. This assumption explains the experimentally observed dependences of the relaxation time on NO $_2$ pressure and ZnO layer thickness, viz. $\tau \sim 1/p(\text{NO}_2)$ and $\tau \sim \exp d_{\text{ZnO}}$ [15]. Disregarding these prefactors leads to an unrealistically small value for the capture cross section.

When we investigate recovery all free carriers are exhausted. Therefore, retrapping can be disregarded. The emission rate from the traps is now mostly determined by the trap depth and by the number of filled traps N_t . The emission rate is given by [30]:

$$e_n = [N_t f(E_t)] v_{th} \sigma_n n_i \exp \left(\frac{E_t - E_i}{kT} \right) \quad (7)$$

Contrary to the temperature independent charge trapping, the recovery is strongly thermally activated. From the temperature dependent recovery experiments we have extracted an activation energy of 1.2 eV, in good agreement with the trap depth of 0.9 eV as derived from the TSC measurements. Detrapping can be described as a simple phonon assisted process. The value of the extracted attempt-to-escape frequency of about 10^{11} Hz is comparable to that of a typical phonon frequency and the capture cross section of 10^{-16} cm 2 is in line with that of a neutral trap.

6. Functional NO₂ sensor

An NO₂ sensor should respond in real time to the partial NO₂ pressure. The threshold voltage of a transistor, biased in accumulation, changes when exposed to NO₂. The change of the threshold voltage with time depends on the partial NO₂ pressure. Hence it seems obvious to make an NO₂ sensor. However, development of a sensor protocol that allows for a dynamic response is not trivial.

Assume we apply a continuous gate bias. Then the threshold voltage shifts to the applied gate bias. The time needed to reach the final state is dependent on the partial NO₂ pressure. However, the final state itself is irrespective of the partial NO₂ pressure and the temperature. Hence, with a fixed continuous gate bias a transistor cannot be used as a sensor. The gate has to be turned on intermittently. When a gate bias is applied the transistor is charged and the threshold voltage shifts. When the transistor is turned off by applying 0 V gate bias, the transistor recovers. By optimizing the cycle time and temperature, the final threshold voltage depends on the partial NO₂ pressure, yielding a real-time NO₂ sensor.

At room temperature a practical sensor cannot be realized. Fig. 2b shows that the time to recover is then in the order of months. Because there is no relaxation, the sensor can only be used once and has to be reset into the pristine state after each measurement. For a dynamic read out the time scales for charging and recovery should be comparable, which can be achieved using higher operating temperatures.

To set the operating temperature and the cycle times we modeled the temporal behavior of the threshold voltage. The response of the transistor can be calculated with experimentally determined parameters, without the use of any additional fit parameters. The model uses the temporal behavior of the threshold voltage as a function of temperature and NO₂ pressure as derived in Section 3. The threshold voltage shifts for trapping and release follow a stretched-exponential time dependence (Eq. (1)). The relaxation times are thermally activated (Eq. (2)). The experimentally determined values for activation energy, attempt-to-escape frequency, and characteristic temperature for both charging and recovery remain fixed. In order to calculate the dependence on NO₂ pressure, the relaxation time for trapping is taken inversely proportional to the NO₂ pressure, as determined previously [15]. The temporal behavior of the sensor can now analytically be calculated.

The operation mechanism of the sensor is elucidated in Fig. 6. For this example the driving protocol consists of repetitive cycles of 10 s charging at a gate bias of 30 V followed by 10 s recovering at a gate bias of 0 V, as presented by the dashed lines. The calculated threshold voltage response is shown for 100 and 1000 ppb NO₂. In the calculation, the bias, V_0 , is taken as the difference between the applied gate bias and the threshold voltage at the start of the pulse. Fig. 6a shows the calculated temporal behavior at room temperature. Upon application of the first gate bias pulse the threshold voltage shifts. Upon switching off the gate bias, the threshold voltage remains unchanged. At room temperature there is no relaxation. In the next charging pulse the threshold shifts further. After infinite time, the threshold voltage is the same as the applied gate bias, irrespective of the NO₂ concentration. The only difference is the time needed to reach the final stage. The transistor acts as an integrator. The threshold voltage irreversibly saturates at the maximum applied gate bias. Fig. 6b shows that by adjusting the operation temperature, a reversible response can be obtained. The threshold voltage shifts upward and downward upon charging and recovering. The selected driving protocol yields a dynamic response where the final threshold voltage is a function of the NO₂ pressure.

The calculated temporal behavior can be understood as follows. The driving force for the change in threshold voltage is the difference between gate bias and the threshold voltage at the start

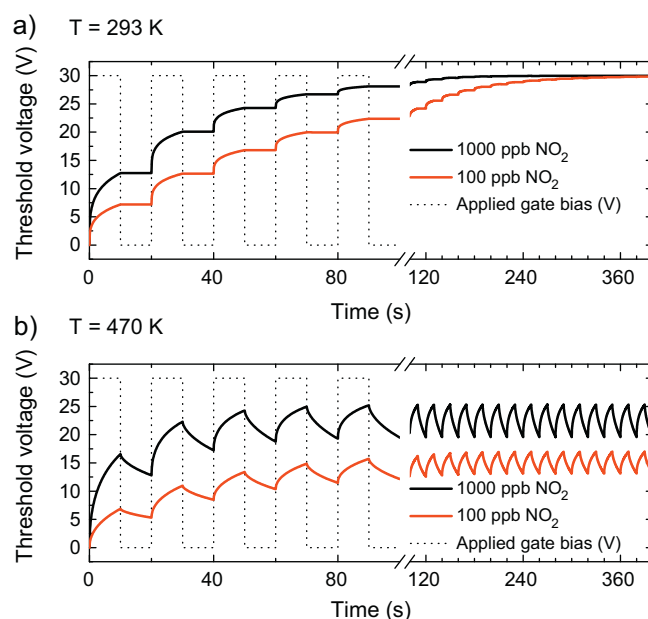


Fig. 6. Calculated threshold voltage response to repetitive cycles of 10 s charging at gate bias 30 V followed by 10 s recovering at gate bias 0 V upon exposure to 100 and 1000 ppb NO₂. (a) At room temperature there is no recovery and for every concentration the threshold voltage saturates at the maximum applied gate bias. (b) At 470 K, the response is reversible and the threshold voltage shifts upward and downward upon charging and recovering. After a number of cycles, a dynamic equilibrium is reached. The maximum and minimum threshold voltages in equilibrium depend on the partial NO₂ pressure.

of the pulse. With an increasing number of cycles, the threshold voltage shifts to the applied gate bias. The driving force for charging decreases and, at the same time, the driving force for recovery increases. Fig. 6b shows that after a number of cycles, ΔV_{th} charging is equal to ΔV_{th} recovery and a dynamic equilibrium is reached. The maximum and minimum threshold voltages in equilibrium increase with partial NO₂ pressure. The concentration dependence follows from the fact that the rate of charging increases with NO₂ pressure while the rate of recovery remains the same.

Using our analytical description, we can calculate the final threshold voltages for each driving protocol, temperature and NO₂ pressure. As an example in Fig. 7 the calculated maximum threshold voltages in equilibrium are presented as a function of NO₂

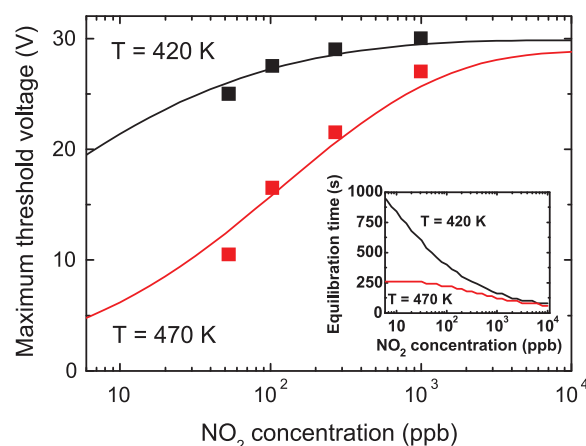


Fig. 7. The maximum threshold voltages in equilibrium after charging as a function of NO₂ content for 420 and 470 K using the driving protocol as in Fig. 6. The solid lines are calculated. The experimentally determined threshold voltages verify the calculations. In the inset the equilibration time is plotted for the specified concentration range.

pressure for 420 K and 470 K. The driving protocol comprised a charge and reset time of 10 s each. The solid lines are calculated. The experimentally determined threshold voltages are presented by the squares. The values coincide with the calculated line. The perfect agreement verifies the methodology developed.

The inset of Fig. 7 shows the time calculated to reach dynamic equilibrium for the specified concentration range. The equilibrium is reached faster at higher temperatures and at higher NO₂ pressure. The reason can be that at higher pressures the rate of charging increases, leading to a faster equilibrium. The calculated equilibrium times have to be compared with those using a driving protocol with full recovery. At 470 K full recovery will take an hour which is incompatible with any practical sensor application. Here we have shown that full recovery is not needed to achieve an NO₂ concentration dependent response. A functional NO₂ sensor can be made by intermittently addressing the gate bias.

We note that a practical sensor can only be obtained by measuring in real sensor's working conditions; changing background conditions should not affect the sensor performance [1]. The selectivity of our sensor towards humidity and other interfering gases has not yet been investigated. Determination of the selectivity is a topic of ongoing research.

The analytical description can be used to optimize the driving protocol. The input parameters follow from the threshold voltage dynamics. Without any fit constants the sensor response can be predicted. By adjusting the driving protocol and operating temperature, the response time can be optimized and the sensitivity can be maximized for the desired partial NO₂ pressure window.

7. Conclusions

The threshold voltage of a field-effect transistor biased in accumulation shifts upon exposure to NO₂. The origin of the shift is charge carrier trapping. The dynamics of trapping and recovery have been investigated as a function of temperature. The obtained functional dependence is used as input for an analytical model that predicts the sensors temporal behavior. The model is experimentally verified and a real-time sensor has been developed.

The NO₂ sensor is based on a field-effect transistor using ZnO as a semiconductor. The ZnO transistors are chemically stable in NO₂. The transport only changes when in an NO₂ ambient a gate bias is applied; the threshold voltage shifts towards the applied gate bias. Charging and recovery measurements have been performed as a function of temperature. The threshold voltage shifts for both trapping and recovery follow a stretched-exponential time dependence. The relaxation times are thermally activated. The activation energies for trapping and release are independent of the NO₂ content and have been determined as 0.1 eV and 1.2 eV respectively. The attempt-to-escape frequency and characteristic temperature have been determined as 1 Hz and 960 K for charge trapping and 10¹¹ Hz and 750 K for recovery.

To confirm the presence of trapped charge carriers and to determine the trap depth, thermally stimulated currents measurements have been performed. The TSC curves have been analyzed, and a trap depth around 1 eV has been obtained. The value is in good agreement with the activation energy derived from the threshold voltage dynamics. Detrapping can be described as a simple phonon assisted process. The value of the extracted attempt-to-escape frequency of about 10¹¹ Hz is comparable to that of a typical phonon frequency and the capture cross section of 10⁻¹⁶ cm⁻² is in line with that of a neutral trap.

For an NO₂ sensor that monitors the partial NO₂ pressure in real time, a sensor protocol has been developed that allows for a dynamic response. The gate bias is turned on intermittently for repetitive cycles of charging and resetting. To obtain comparable

time scales for trapping and detrapping, higher operating temperatures are used. The threshold voltage shifts upward and downward upon charging and recovering. A dynamic equilibrium is reached where the final threshold voltage is a function of the partial NO₂ pressure. To set the operating temperature and the driving protocol we have analytically calculated the temporal behavior of the threshold voltage, using the experimentally determined parameters from the charging and recovery measurements as input. The response of the transistor can be calculated without any additional fit constants. The methodology has been verified by comparing the calculated values with experimentally determining values. The perfect agreement validates the methodology developed. The analytical description can be used to optimize the driving protocol. By adjusting the duration of charging and resetting and the operating temperature, the response time can be optimized and the sensitivity can be maximized for the desired NO₂ concentration window.

Acknowledgements

We gratefully acknowledge technical assistance from H. Verberne and T.C.T. Geuns from MiPlaza, Eindhoven, and financial support from the Zernike Institute for Advanced Materials, the Netherlands Organization for Scientific Research (NWO, Vidi grant) and from the EU (project ONE-P no. 212311).

References

- [1] N. Barsan, D. Koziej, U. Weimar, Metal oxide-based gas sensor research: how to? *Sensors and Actuators B* 121 (2007) 18–35.
- [2] N. Barsan, U. Weimar, Conduction model of metal oxide gas sensors, *Journal of Electroceramics* 7 (2001) 143–167.
- [3] T. Inoue, K. Ohtsuka, Y. Yoshida, Y. Matsuura, Y. Kajiyama, Metal oxide semiconductor NO₂ sensor, *Sensors and Actuators B* 25 (1995) 388–391.
- [4] L. Torsi, A. Dodabalapur, Organic thin-film transistors as plastic analytical sensors, *Analytical Chemistry* 77 (2005) 380A–387A.
- [5] M.E. Roberts, A.N. Sokolov, Z. Bao, Material and device considerations for organic thin-film transistor sensors, *Journal of Materials Chemistry* 19 (2009) 3351–3363.
- [6] A. Das, R. Dost, T. Richardson, M. Grell, J.J. Morrison, M.L. Turner, A nitrogen dioxide sensor based on an organic transistor constructed from amorphous semiconducting polymers, *Advanced Materials* 19 (2007) 4018–4023.
- [7] F. Marinelli, A. Dell'Aquila, L. Torsi, J. Tey, G.P. Suranna, P. Mastrorilli, G. Romanazzi, C.F. Nobile, S.G. Mhaisalkar, N. Cioffi, F. Palmisano, An organic field effect transistor as a selective NO₂ sensor operated at room temperature, *Sensors and Actuators B* 140 (2009) 445–450.
- [8] G. Barillaro, A. Diligenti, A. Nannini, L.M. Strambini, E. Comini, G. Sberveglieri, Low-concentration NO₂ detection with an adsorption porous silicon FET, *IEEE Sensors Journal* 6 (2006) 19–23.
- [9] G. Barillaro, L.M. Strambini, An integrated CMOS sensing chip for NO₂ detection, *Sensors and Actuators B* 134 (2008) 585–590.
- [10] M.C. McAlpine, H. Ahmad, D.W. Wang, J.R. Heath, Highly ordered nanowire arrays on plastic substrates for ultrasensitive flexible chemical sensors, *Nature Materials* 6 (2007) 379–384.
- [11] J. Kong, N.R. Franklin, C.W. Zhou, M.G. Chapline, S. Peng, K.J. Cho, H.J. Dai, Nanotube molecular wires as chemical sensors, *Science* 287 (2000) 622–625.
- [12] T. Helbling, R. Pohle, L. Durrer, C. Stampfer, C. Roman, A. Jungen, A. Fleischer, C. Hierold, Sensing NO₂ with individual suspended single-walled carbon nanotubes, *Sensors and Actuators B* 132 (2008) 491–497.
- [13] O. Kuzmych, B.L. Allen, A. Star, Carbon nanotube sensors for exhaled breath components, *Nanotechnology* 18 (2007) 375502.
- [14] D.H. Zhang, Z.Q. Liu, C. Li, T. Tang, X.L. Liu, S. Han, B. Lei, C.W. Zhou, Detection of NO₂ down to ppb levels using individual and multiple In₂O₃ nanowire devices, *Nano Letters* 4 (2004) 1919–1924.
- [15] A. Andringa, J.R. Meijboom, E.C.P. Smits, S.G.J. Mathijssen, P.W.M. Blom, D.M. de Leeuw, Gate-bias controlled charge trapping as a mechanism for NO₂ detection with field-effect transistors, *Advanced Functional Materials* 21 (2011) 100–107.
- [16] The difference between the switch-on voltage and the threshold voltage can be disregarded, since the shift of both parameters is equal.
- [17] A. Bashir, P.H. Wobkenberg, J. Smith, J.M. Ball, G. Adamopoulos, D.D.C. Bradley, T.D. Anthopoulos, High-performance zinc oxide transistors and circuits fabricated by spray pyrolysis in ambient atmosphere, *Advanced Materials* 21 (2009) 2226–2231.
- [18] D.A. Jones, J.U. Lee, Observation of the Urbach tail in the effective density of states in carbon nanotubes, *Nano Letters* 11 (2011) 4176–4179.

- [19] G.Y. Lu, J. Xu, J.B. Sun, Y.S. Yu, Y.Q. Zhang, F.M. Liu, UV-enhanced room temperature NO₂ sensor using ZnO nanorods modified with SnO₂ nanoparticles, *Sensors and Actuators B* 162 (2012) 82–88.
- [20] J.D. Prades, R. Jimenez-Diaz, F. Hernandez-Ramirez, S. Barth, A. Cirera, A. Romano-Rodriguez, S. Mathur, J.R. Morante, Equivalence between thermal and room temperature UV light-modulated responses of gas sensors based on individual SnO₂ nanowires, *Sensors and Actuators B* 140 (2009) 337–341.
- [21] E. Comini, G. Faglia, G. Sberveglieri, UV light activation of tin oxide thin films for NO₂ sensing at low temperatures, *Sensors and Actuators B* 78 (2001) 73–77.
- [22] A. Sharma, S.G.J. Mathijssen, E.C.P. Smits, M. Kemerink, D.M. de Leeuw, P.A. Bobbert, Proton migration mechanism for operational instabilities in organic field-effect transistors, *Physical Review B* 82 (2010), 075322.
- [23] C. Casteleiro, H.L. Gomes, P. Stallinga, L. Bentes, R. Ayouchi, R. Schwarz, Study of trap states in zinc oxide (ZnO) thin films for electronic applications, *Journal of Non-Crystalline Solids* 354 (2008) 2519–2522.
- [24] R. Chen, Y. Kirsh, *Analysis of Thermally Stimulated Processes*, 1st ed., Pergamon Press, Oxford, 1981.
- [25] P. Blood, J.W. Orton, The electrical characterisation of semiconductors, *Reports on Progress in Physics* 41 (1978) 157–257.
- [26] P. Blood, J.W. Orton, *The Electrical Characterization of Semiconductors: Majority Carriers and Electron States*, Academic Press, New York, 1992.
- [27] M. Meier, S. Karg, K. Zuleeg, W. Brütting, M. Schwoerer, Determination of trapping parameters in poly(p-phenylenevinylene) light-emitting devices using thermally stimulated currents, *Journal of Applied Physics* 84 (1998) 87–92.
- [28] T.A.T. Cowell, J. Woods, The evaluation of thermally stimulated current curves, *British Journal of Applied Physics* 18 (1967) 1045–1051.
- [29] S. Nakabayashi, A. Kira, M. Ipponmatsu, Dynamic photocapacitance measurement of zinc oxide photoelectrode in aqueous solution, *Journal of Physical Chemistry* 93 (1989) 5543–5548.
- [30] R.S. Muller, T.I. Kamins, *Device Electronics for Integrated Circuits*, 2nd ed., John Wiley & Sons, New York, 1986.

Biographies

Anne-Marije Andringa was born in Akkrum, The Netherlands, in 1984. She received the B.Sc. and M.Sc. degrees in chemistry from the University of Groningen, Groningen, The Netherlands, in 2005 and 2008, respectively. She is currently working toward the Ph.D. degree in the group Physics of Organic Semiconductors, Zernike Institute for Advanced Materials, University of Groningen, and in the group Photonic Materials and Devices, Philips Research Laboratories, Eindhoven. Her research focuses on the use of field-effect transistors in sensor applications.

Nynke Vlietstra received her B.Sc. and M.Sc. degree in Applied Physics in 2009 and 2011, respectively, from the University of Groningen, Groningen, The Netherlands. As a part of her master program, she worked at Philips Research Laboratories, where she did research on gas sensing using field-effect transistors. After her graduation, she started her Ph.D. at the University of Groningen at the Zernike Institute for Advanced Materials, in the group 'Physics of Nanodevices'. She is currently working in the field of (metallic) spintronics, where she investigates the creation, detection and control of spin currents in mostly metallic devices.

Edsger C.P. Smits was born in Huizen, The Netherlands, in 1979. He received his M.Sc. in 2004 and his Ph.D. degree cum laude in 2009 from the University of

Groningen, Groningen, The Netherlands. In his Ph.D. study, he investigated ambipolar and self-assembled monolayer organic field effect transistors. Since 2009, he has been a Researcher with Holst Centre, Eindhoven, The Netherlands, which is a joint research initiative of Dutch Organization for Applied Scientific Research (TNO) and IMEC, in the technology program called "Sensor Tags and Systems". He is the author and co-author of more than 30 publications in peer-reviewed journals and book chapters. His main research interests are novel fabrication processes of organic and oxide thin-film transistors and hybrid integration solutions for RFID sensor tags.

Mark-Jan Spijckman was born in Drachten, The Netherlands, in 1982. He received his M.Sc. degree in Applied Physics in 2007 and his Ph.D. degree in 2011, both from the University of Groningen, Groningen, The Netherlands. The Ph.D. research focussed on the application of organic semiconductors in logic circuits and for sensing applications, with a focus on dual-gate transistors. The Ph.D. was performed at Philips Research Laboratories, Eindhoven, The Netherlands. Currently he works as a postdoctoral researcher in the same group on organic ferroelectric memories.

Henrique Leonel Gomes was born in Monte-Real, Portugal, in 1963. He received his B.Sc. degree in Physics from the University of Aveiro, Portugal. He earned his Ph.D. in Electronic Engineering in 1994 from University College of North Wales, UK, for work on the electrical properties of semiconducting organic thin films. He moved to the University of the Algarve, Portugal, where he is Associate Professor in the Electronics Engineering department. His research interests have always been directed towards the electrical characterisation of thin film electronic devices such as field effect transistors, diodes and MIS capacitor structures.

Johan H. Klootwijk received the M.Sc. and Ph.D. degrees in electrical engineering from the University of Twente, Enschede, The Netherlands, in 1993 and 1997, respectively. He then joined Philips Research Laboratories, Eindhoven, where his work covers a wide range of applications, a.o. wideband RF applications, nanowire sensors, EUV spectral purity filters and new materials for direct conversion CT scanners. Dr. Klootwijk received the Best Paper Award for on the ESSDERC Conference in 2001 and a Bronze Award for the 'NXP Invention of the Year 2007'. He served as the Tutorial Chairman of the International Conference on Measurement and Teststructures, ICMTS, 2002, 2008 and 2011.

Paul W.M. Blom, born in 1965 in The Netherlands, received his Ph.D. degree in 1992 from the Technical University Eindhoven on picosecond charge carrier dynamics in GaAs. At Philips Research Laboratories he was engaged in the electro-optical properties of polymer light-emitting diodes. From 2000 he held a professorship at the University of Groningen in the field of electrical and optical properties of organic semiconducting devices. In September 2008 he became Scientific Director of the Holst Centre in Eindhoven, where the focus is on foil-based electronics, followed in 2012 by an appointment as director at the MPI for polymer research.

Dago de Leeuw is a research fellow at Philips Research Laboratories, Eindhoven, The Netherlands, and professor in Molecular Electronics at the University of Groningen, The Netherlands. His Ph.D. degree was obtained at the Free University of Amsterdam in 1979 on "Helium (I) photoelectron spectroscopy of transient species". He has worked on materials science and technology of phosphors, high-Tc superconductors, laser ablation, ferroelectrics and polymer electronics. The activities have led to 30 US patents and 230 regular papers. The work on plastic electronics has been rewarded with the Discover Awards in 1999 and the Descartes Prize in 2000. His whole work was rewarded by Philips Research with the Gilles Holst award in 2004. His current research interests are molecular electronics, non-volatile data storage, LEDs and biosensors.